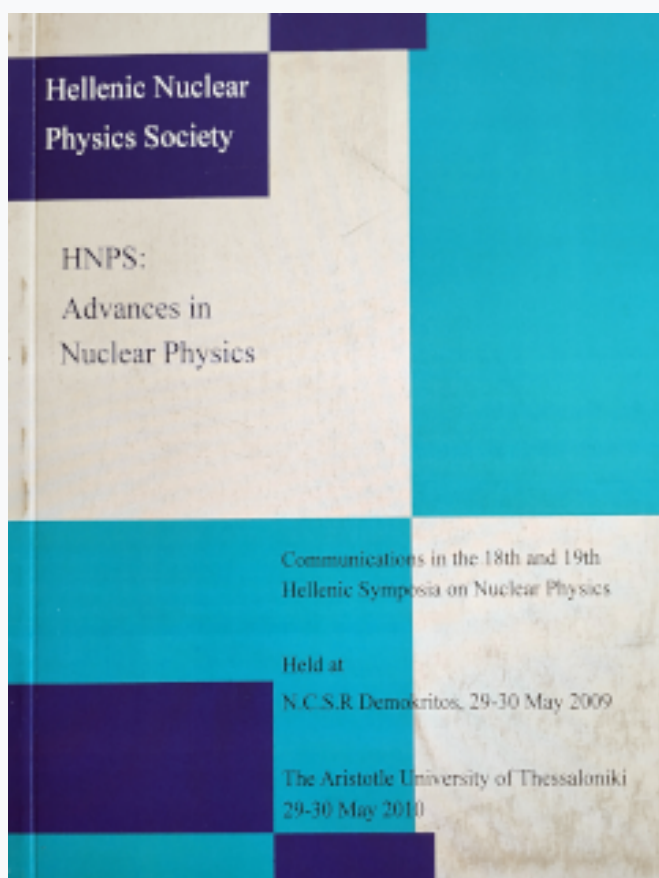


HNPS Advances in Nuclear Physics

Vol 17 (2009)

HNPS2009



Experimental study of the $^{197}\text{Au}(n,2n)$ reaction cross section

A. Tsinganis, M. Kokkoris, A. Lagoyannis, E. Mara, C. T. Papadopoulos, R. Vlastou

doi: [10.12681/hnps.2565](https://doi.org/10.12681/hnps.2565)

To cite this article:

Tsinganis, A., Kokkoris, M., Lagoyannis, A., Mara, E., Papadopoulos, C. T., & Vlastou, R. (2019). Experimental study of the $^{197}\text{Au}(n,2n)$ reaction cross section. *HNPS Advances in Nuclear Physics*, 17, 9–14.
<https://doi.org/10.12681/hnps.2565>

Experimental study of the $^{197}\text{Au}(n,2n)$ reaction cross section

A. Tsinganis^a, M. Kokkoris^a, A. Lagoyannis^b, E. Mara^a, C. T. Papadopoulos^a, R. Vlastou^a

^a*Department of Physics, National Technical University of Athens, Greece*

^b*Institute of Nuclear Physics, NCSR “Demokritos”, Athens, Greece*

Abstract

In the present work, the $^{197}\text{Au}(n,2n)$ reaction cross section is experimentally determined relative to the $^{27}\text{Al}(n,\alpha)^{24}\text{Na}$ reaction at incident neutron energies of 9.0 to 10.5 MeV by means of the activation technique. The quasi-monoenergetic fast neutron beam was produced via the $^2\text{H}(d,n)^3\text{He}$ reaction at the 5.5 MV Tandem Van de Graaff accelerator at the NCSR “Demokritos” and was studied to determine the contribution of background “parasitic” neutrons using the multiple foil activation technique and the SULSA unfolding code. The cross sections for the population of the second isomeric state (12^-) of ^{196}Au and the sum of the ground (2^-) and first isomeric state (5^-) population cross sections were independently determined. Auxiliary Monte Carlo simulations were performed with the MCNP code.

1. Introduction

The presence of a high spin isomeric state in the residual nucleus of a neutron threshold reaction provides a sensitive test for existing nuclear models. The systematic study of the excitation function of the formation of both the ground and the high spin isomeric state on the basis of a statistical model provides information on the energy and spin distribution of the level density of the nuclei involved [1] and on the changes in the structure of the low lying excited states of the corresponding nuclei.

In this context the ^{196}Au isotope presents an interesting isomeric pair: ground and isomeric states with spin values of 2^- and 12^- respectively (Fig. 1). This 12^- isomer has been reported for other even A Au isotopes (^{198}Au , ^{200}Au) [2]. However, a survey of the literature revealed only a limited number of experimental data for the cross section of the $^{197}\text{Au}(n,2n)^{196}\text{Au}^{m2}$ reaction, especially near its threshold, where only one unpublished dataset [3] was found.

Thus, the purpose of this work was to experimentally determine the $^{197}\text{Au}(n,2n)^{196}\text{Au}^{m2}$ and the $^{197}\text{Au}(n,2n)^{196}\text{Au}^{g+m1}$ reaction cross sections in the incident neutron energy range between 9 and 10.5 MeV, i.e. close to the threshold, by means of the activation technique, with the view of conducting a detailed theoretical study of these cross-sections in the near future.

2. Experimental

2.1. Irradiations

Four irradiations have been carried out, evenly spaced in the energy range between 9.0 to 10.5 MeV. Given that the cross section for the formation of the second isomeric state is significantly lower than that for the population of the ground state, the irradiations typically lasted approximately 24 hours, which corresponds to roughly 84% of the saturated activity of the second isomeric state.

High purity natural gold foils (99.99% ^{197}Au) with a diameter of 14 mm and thickness of 0.5 mm were used. Two Al foils of the same diameter and thickness were placed immediately before and after the gold foil and were used to determine the neutron flux.

The quasi-monoenergetic neutron beam was produced via the $^2\text{H}(d,n)^3\text{He}$ reaction by bombarding a deuterium gas target with a deuteron beam at currents around 1-2 μA . The gas target is fitted with a 5 μm molybdenum entrance foil and a 1 mm Pt beam stop and is constantly cooled with a cold air jet during

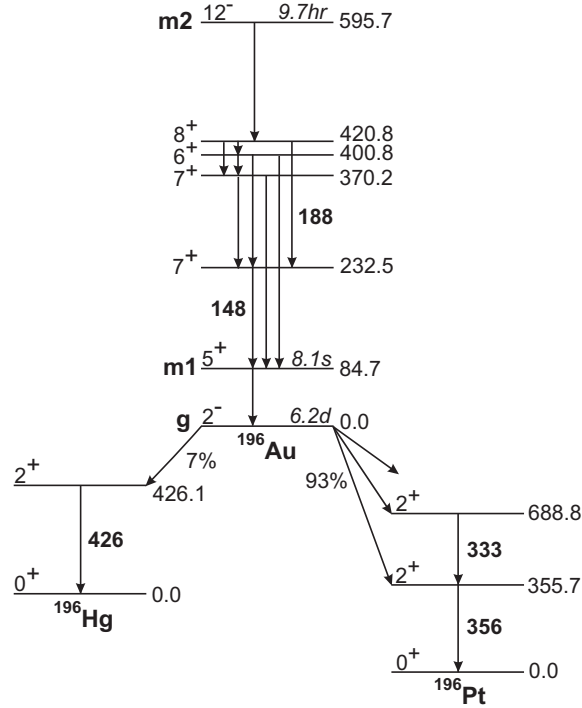


Figure 1: Simplified decay scheme of the isomeric and ground states of the residual nucleus ^{196}Au . All energies are given in keV.

irradiation to diminish the risk of damage to the Mo foil. The deuterium pressure was set to 1500 mbar. Using this setup, the achieved flux varied between 3×10^5 - 4×10^6 n/(cm²·s) in the four runs performed.

The samples were placed at 0° with respect to the neutron beam and at a distance of 8 cm from the center of the gas cell, thus limiting the angular acceptance of the target foils to $\pm 5^\circ$.

Beam fluctuations were monitored with a BF_3 counter placed at a distance of 3 m from the deuterium gas target. Following Monte Carlo simulations of the experimental area, the BF_3 unit was placed at an angle of 30° with respect to the beam line to avoid an increased presence of “parasitic” background neutrons near the target foils due to backscattering on the BF_3 setup. Data from the BF_3 counter were stored at regular time intervals (60 s) by means of a multi-channel scaler and were used to correct for the decay of ^{196}Au nuclei during irradiation and to account for fluctuations in the beam flux in the subsequent off-line analysis.

2.2. Neutron Beam

Particular attention was given to estimating the neutron energy distribution in the samples. The linearity of the selection magnet has been verified at low energies through the $\text{Al}(p,\gamma)$ strong resonance at 991.91 keV and the $^{16}\text{O}(d,n)$ threshold reaction ($E_{th}=1828.83$ keV) leading to an estimate of the beam energy offset of 1.6 keV and a beam energy uncertainty of 0.1%. Assuming possible non-linearity at high energies, an overestimated beam energy uncertainty of 0.15% has been accepted to include possible second order effects.

A considerably more significant effect on the energy uncertainty of the produced neutrons is straggling from energy loss in the entrance foil and the deuterium target. Furthermore, as it was not possible to control the flow of deuterium in the gas cell remotely, the pressure was at times lower than the desired value by up to 200-300 mbar. These effects were estimated with the SRIM software [4] and the energy uncertainty value from straggling was less than 30 keV. Finally, the angular acceptance of the target foils introduces additional uncertainty due to the $^2\text{H}(d,n)^3\text{He}$ reaction kinematics.

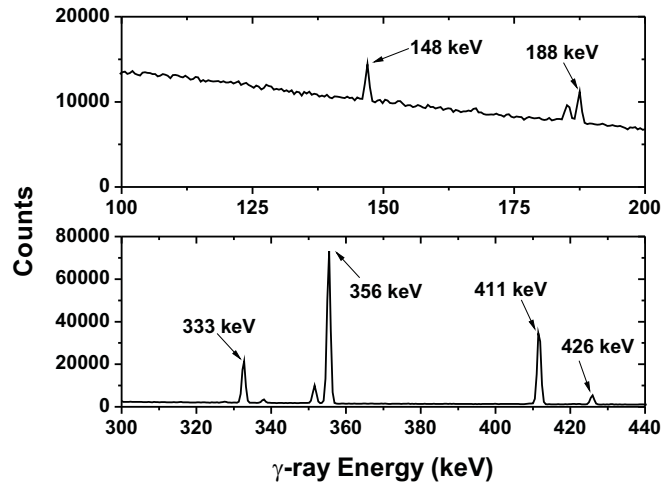


Figure 2: Experimental spectra from the decay of the second isomeric state (top panel) and ground state (bottom panel) of ^{196}Au , after irradiation at 10.5 MeV incident neutron energy. The acquisition time is 20hr and 51hr respectively.

Taking the above into account, the appropriate adjustments were made, where possible, to ensure that the width of the neutron energy distribution in the samples did not exceed 50keV.

The contribution of background “parasitic” neutrons was also studied in detail. These neutrons originate from the interaction of the deuteron beam with the beam line structural materials, beam collimators and gas cell components. The multiple foil activation technique was implemented to determine the neutron beam profile. The appropriate foils (Ni, Co, Ti, In, Zn, Fe, Nb) were chosen in which neutron threshold reactions take place at different threshold energies and they were placed immediately after the Au and two Al foils for irradiation. Information from the Au and Al foils was also included in this analysis.

The results of these irradiations were processed with the SULSA unfolding code [5]. By providing the activation rates measured for each foil, the code extrapolates the energy distribution of the beam using cross section values and covariance matrices from an incorporated library. Modifications were made to include additional reactions in the analysis.

The results of this analysis showed that, although a considerable population of background neutrons is produced during the irradiations, these lie mainly in the low-energy region, well below the threshold for the $^{197}\text{Au}(n,2n)$ ($E_{th} = 8.11$ MeV) reaction. As far as the $^{27}\text{Al}(n,\alpha)^{24}\text{Na}$ reference reaction is concerned, while $E_{th} = 3.25$ MeV, the cross section only grows sufficiently to produce measurable activation rates at incident neutron energies above 6.8 MeV.

2.3. Activity Measurements

Following the irradiations, the induced activity on the samples was measured with a 56% relative efficiency HPGe detector. The detector was calibrated with ^{152}Eu and ^{207}Bi sources, the latter being used to obtain a more accurate efficiency curve in the low-energy region. The samples were placed at a distance of 10 cm from the detector window. With this counting setup, corrections for coincidence summing become negligible. Figure 2 shows typical spectra acquired from the gold samples during the measurement for the second isomeric state (top panel) and the ground state (bottom panel), where the γ -rays of interest have been marked.

The population of the second isomeric state was measured through the 148 keV line. This was preferred over the 188 keV line due to its higher intensity (45% over 30%) and the existence of a nearby natural background line (Fig. 2). These measurements began approximately 1 hr after the end of the irradiation and lasted up to 20 hr (two half-lives), depending on the evolution of the peak-to-background ratio. Following this, the activity of the Al foils was measured with the same experimental setup through the 1369 keV transition. For these measurements, a duration between 1 and 3 hr was sufficient to achieve a statistical error lower than 2%.

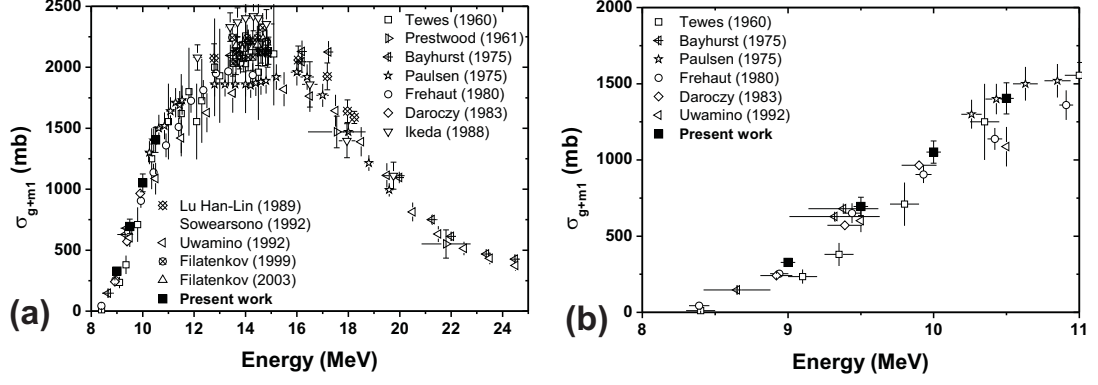


Figure 3: Experimental cross section values for the population of the ground and first isomeric state of ^{196}Au (g+m1) between 8-25 MeV (a) and 8-11 MeV (b). Several single-point datasets around 14 MeV omitted for clarity.

Since the first isomeric state decays relatively very quickly ($T_{1/2} = 8.1$ s), the measurements on the decay of the ground state result in the determination of the sum of the cross sections for the population of the ground state and the first isomeric state. Moreover, these measurements were carried out at least two days after the irradiation to ensure that the second isomeric state ($T_{1/2} = 9.6$ hr) had fully decayed to the ground state, since the correction for the contribution of the second isomeric state to the measured activity of the ground state was found to be negligible when the latter measurement was carried out after several half-lives of the second isomeric state.

The activity of the ground state was deduced through the 356 keV line, preferred over the 333- and 426 keV lines due to the much higher counting statistics (Fig. 2). Furthermore, the 333 keV line is contaminated by the 334 keV line of ^{198}Au arising from the $^{197}\text{Au}(n,\gamma)^{198}\text{Au}$ reaction. This is confirmed by the 411 keV line which is clearly visible in the acquired spectrum and also belongs to the (n, γ) channel.

3. Data Analysis

In each case, the experimental values of the cross sections were determined through the following formula:

$$\sigma = \frac{N_\gamma}{\epsilon I N_T \Phi S f D} \quad (1)$$

where N_γ is the number of counts in the relevant γ -ray peak. The factor ϵ is the detector efficiency, I is the γ -ray intensity, N_T is the number of target nuclei and S is the self-absorption correction factor. Decays during irradiation and time fluctuations in the beam flux are accounted for with the correction factor f , given by:

$$f = \frac{\int_0^{t_b} e^{-\lambda t} F(t) dt}{\int_0^{t_b} F(t) dt} e^{-\lambda t_b}, \quad (2)$$

where t_b is the irradiation time and $F(t)$ is the beam flux in arbitrary units as given by the BF_3 counter, while D corrects for the interval between the end of the irradiation and the end of the measurement and is given by:

$$D = (1 - e^{-\lambda t_m}) e^{-\lambda t_w}, \quad (3)$$

where t_w and t_m are the waiting time between irradiation and measurement and the measurement time respectively.

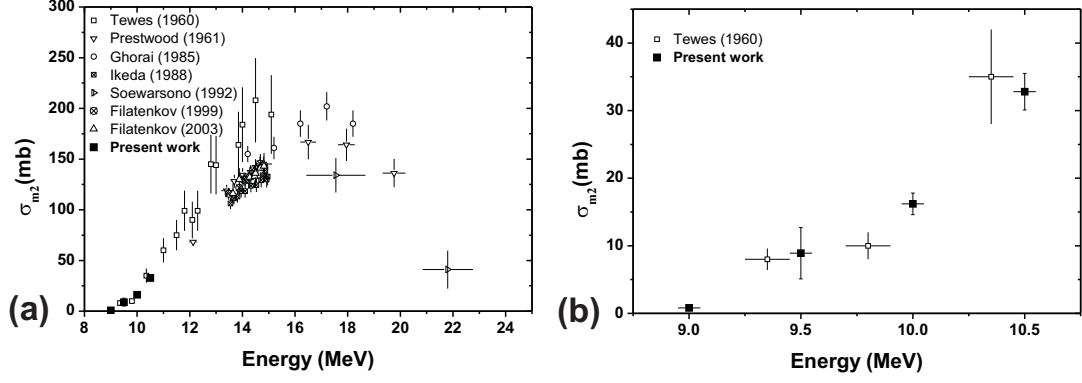


Figure 4: Experimental cross section values for the population of the second isomeric state of ^{196}Au (m_2) between 8-25 MeV (a) and 8.5-11 MeV (b).

Table 1: Experimental cross section values for the $^{197}\text{Au}(n,2n)^{196}\text{Au}^{g+m1}$ and $^{197}\text{Au}(n,2n)^{196}\text{Au}^{m2}$ reactions and the isomeric cross section ratio

Energy (MeV)	σ_{g+m1} (mb)	σ_{m2} (mb)	$\sigma_{m2}/\sigma_{g+m1}$
9.0	328 ± 26	0.8 ± 0.1	0.0024 ± 0.0003
9.5	695 ± 60	8.9 ± 3.8	0.013 ± 0.006
10.0	1052 ± 73	16.2 ± 1.6	0.015 ± 0.002
10.5	1404 ± 102	32.8 ± 2.7	0.023 ± 0.003

The integrated neutron flux Φ was determined through the same formula (Eq. 1) by using the cross section values for the $^{27}\text{Al}(n,\alpha)^{24}\text{Na}$ reaction found in literature [6] and by averaging over the deduced values in the front and back Al foils. It is thus possible to correct for target geometry and self-shielding.

Given the relatively low energy of the γ -rays of interest and the high mass attenuation coefficient of gold, it was essential to take self-absorption effects into consideration. A Monte Carlo simulation of the counting geometry using the MCNP code [7] was performed to estimate this correction. Approximately 55% of the 148 keV and 12% of the 356 keV line are lost due to self-absorption in a 0.5 mm -thick gold foil. Self-absorption of the 1369 keV line in Al was found to be less than 0.5%.

4. Results and Discussion

The experimental results of this work are presented in Table 1 along with their uncertainties. As seen in figure 3, the data for the $^{197}\text{Au}(n,2n)^{196}\text{Au}^{g+m1}$ cross section are in good agreement with previous measurements.

For the second isomeric state, only one previous dataset exists in the energy region from threshold to 13 MeV, contained in an unpublished report [3]. It has been impossible to obtain relevant information on the particular experiment, such as beam parameters, flux, irradiation intervals and the detector(s) used for the off-line measurements. A dataset of evaluated data in this region can additionally be found in [8], also an unpublished report. The new data presented in this work report significantly lower uncertainties (10-11% for the 10.0 and 10.5 MeV measurements compared to 20% in the other data within this range), barring the non-optimal 9.5 MeV measurement. Moreover, the measurement at 9.0 MeV is the only one carried out at this energy, so close to the threshold. The uncertainty in the incident neutron energy has also been reduced compared to the previous data, as described in subsection 2.2.

5. Conclusions

The cross section of the (n,2n) reaction on ^{197}Au , was measured independently for the population of the second isomeric state (σ_{m2}), and for the sum of the reaction cross section for the population of the ground and the first isomeric state (σ_{g+m1}). The cross section values were determined by means of the activation technique in the incident neutron energy range 9.0-10.5 MeV. The present data provide more accurate measurements in the near-threshold region.

6. Acknowledgments

The present work was partially supported by the NTUA program for fundamental research PEVE-2008. The authors would also like to acknowledge the assistance of the accelerator staff at NCSR “Demokritos”.

- [1] Y. P. Gangrsky, N. N. Kolesnikov, V. G. Lukashik, and L. M. Melnikova, *Physics of Atomic Nuclei* **67**, 1227 (2004).
- [2] E. Hagn and E. Zech, *Nucl. Phys. A* **373**, 256 (1982).
- [3] H. A. Tewes, A. A. Caretto, A. E. Miller, and D. R. Nethaway, Tech. Rep. 6028 (USA, 1960) data retrieved from EXFOR: www-nds.iaea.org/exfor.
- [4] J. F. Ziegler, J. P. Biersack, and U. Littmark, *The Stopping and Range of Ions in Solids* (Pergamon Press, New York, 1985).
- [5] S. Sudar, *A Solution for the Neutron Spectrum Unfolding Problem without Using Input Spectrum*, Tech. Rep. INDC(HUN)-026/L (Vienna, 1989).
- [6] A. Carlson, R. Block, J. Briggs, E. Cheng, H. Huria, M. Zerkle, K. Kozier, A. Courcelle, V. Pronyaev, and S. van der Marck, *Nuclear Data Sheets* **107**, 2391 (2006).
- [7] F. B. Brown, R. F. Barrett, T. E. Booth, J. S. Bull, L. J. Cox, R. A. Forster, T. J. Goorley, R. D. Mosteller, S. E. Post, R. E. Prael, E. C. Selcow, A. Sood, and J. Sweezy, *Trans. Am. Nucl. Soc.* **87**, 273 (2002).
- [8] C. Phillis and O. Bersillon, Tech. Rep. 4826 (France, 1977) data retrieved from EXFOR: www-nds.iaea.org/exfor.